Contribution from the Istituto di Chimica Generale e Inorganica, Università,
Laboratorio CNR, Florence, Italy

Transition-Metal Complexes with Sulfur Atom as Ligand. 2.[1] Synthesis, Properties, and Structural Characterization of Thio, Mercapto, and Methylthio Complexes of Cobalt(I) and Nickel(I) and -(II) with Poly(tertiary phosphines)

CARLO MEALLI, STEFANO MIDOLLINI, and LUIGI SACCONI*

Received April 7, 1977

The tri(tertiary phosphines) 1,1,1-tris(diphenylphosphinomethyl)ethane, p_3, and tris(2-diphenylphosphinoethyl)amine, np_3, form dimeric thio complexes of nickel(II) and cobalt(I) with formulas $[(p_3)NiSNi(p_3)](BPh_4)_2 \cdot 1.6DMF$, **1**, and $[(np_3)CoSCo(np_3)]$, **2**, respectively. Two x-ray structural investigations have shown that in both complexes the metal ions are tetrahedrally coordinated to the three phosphorus atoms of the ligand and to the bridging sulfur atom. Crystal data for **1**: space group $P\bar{1}$, $a = 17.754$ (4) Å, $b = 13.972$ (3) Å, $c = 12.658$ (3) Å, $\alpha = 93.09(2)°$, $\beta = 106.41$ (2)°, $\gamma = 106.89$ (2)°, $Z = 1$. Crystal data for **2**: space group $R\bar{3}c$, $a = 24.505$ (4) Å, $\alpha = 31.71$ (3)°, $Z = 2$. Noteworthy in both complexes are the short M–S distances (Ni–S = 2.034 (2) and Co–S = 2.128 (1) Å). In the cobalt complex the apical nitrogen atom is not bound to the metal (Co–N = 3.485 (8) Å). These are the first two examples of diamagnetic d^8 metal complexes in which the metal is tetrahedrally coordinated. The triphosphine np_3 also forms five-coordinate mercapto, methylthio, and hydrogenselenido complexes of nickel(I) with formulas $[NiX(np_3)]$ (X = SH, SCH_3, SeH).

Introduction

It has recently been stated that both bridged and monodentate transition-metal thiols are extremely rare.[2]

We have shown that some tri(tertiary phosphines), e.g., tris(2-diphenylphosphinoethyl)amine, np_3, and tris(2-diphenylphosphinoethyl)phosphine, pp_3, can stabilize transition-metal thiols and, by using these phosphines as coligands, we have been able to prepare five-coordinate complexes of the general formula $[M(SR)L]Y$ (M = Fe, Co, Ni; R = H, CH_3; L = pp_3, np_3; $Y^- = BF_4^-$, BPh_4^-).[1] X-ray structural analyses on some of these compounds have shown them to possess trigonal-bipyramidal structures with the sulfur atom in an axial position.[1]

This ability of the poly(tertiary phosphines) to stabilize metal–thiolo complexes prompted us to extend our research (1) by using other tri(tertiary phosphines), e.g., the potentially tridentate 1,1,1-tris(diphenylphosphinomethyl)ethane, p_3, and (2) by attempting to synthesize mercapto complexes of cobalt and nickel in oxidation state +1.

We have succeeded in preparing two bridged thio complexes of nickel(II) and cobalt(I) with the ligands p_3 and np_3, respectively. Furthermore, we have isolated some mercapto and hydrogenselenido complexes of nickel(I) with np_3.

All complexes have been characterized by appropriate physical methods.

The complete x-ray structural analysis has been carried out on the two thio complexes $[(p_3)NiSNi(p_3)](BPh_4)_2 \cdot 1.6DMF$ and $[(np_3)CoSCo(np_3)]$.

A preliminary account of part of this work has already been published.[3]

Experimental Section

Reagents. Ethanol, 1-butanol, *N,N*-dimethylformamide, methylene chloride, and petroleum ether solvents were of reagent grade quality and were used without further purification; tetrahydrofuran was purified by distillation over $LiAlH_4$. The ligands p_3[4] and np_3[5] and the complexes $[Co(SH)(np_3)]BPh_4$[1] and $[Ni(np_3)]$[6] were prepared by the methods previously described. Hydrogen selenide was prepared by reaction of Al_2Se_3 with H_2O.

Preparation of the Complexes. All preparation operations were carried out under dry nitrogen, using deoxygenated solvents, and the complexes were dried in a stream of dry nitrogen.

$[(p_3)NiSNi(p_3)](BPh_4)_2 \cdot 1.6DMF$. The ligand p_3 (1 mmol) in 10 mL of DMF was added to a solution of $[Ni(H_2O)_6](BF_4)_2$ (1 mmol) in 20 mL of 1-butanol. When H_2S was bubbled through the solution, at room temperature, a deep green color immediately appeared and, after further bubbling of H_2S for 5 min, a solution of $NaBPh_4$ (1 mmol) in 20 mL of 1-butanol was added to the reaction mixture. Dark green crystals slowly separated and were filtered off and washed with 1-butanol and then with petroleum ether.

$[(np_3)CoSCo(np_3)]$. Sodium metal (2.5 mmol) was allowed to react completely with 10 mL of ethanol and the resulting solution of sodium ethoxide was added, at room temperature, to a solution of $[Co(SH)(np_3)]BPh_4$ (1 mmol) in 15 mL of THF. After 3 min, brown crystals appeared which were filtered off and washed first with ethanol and then with petroleum ether.

$[Ni(SH)(np_3)]$. H_2S was bubbled into a solution of $[Ni(np_3)]$ (1 mmol) in 60 mL of THF. After about 10 min, deep brown crystals began to separate from the brown solution and these were filtered off after 2 h and washed with ethanol and petroleum ether.

$[Ni(SeH)(np_3)]$, $[Ni(SCH_3)(np_3)]$. These compounds were prepared by a method analogous to that above using H_2Se and $HSCH_3$ instead of H_2S.

Physical Measurements. The physical measurements were performed by previously described methods.[7] The analytical, magnetic, and conductivity data of the complexes are reported in Table I. Table II lists the electronic spectral data.

Collection and Reduction of X-Ray Intensity Data. Solution and Refinement of the Structures. Both compounds were studied on a PW 1100 Philips fully automated diffractometer using the Mo Kα radiation monochromatized with a flat graphite monochromator crystal. The parameters of the unit cells were obtained and refined from the information gathered using the "peak hunting" procedure[8] after suitable crystals of each compound had been positioned in a random orientation in the center of the instrument. Detailed information about the experimental and computational work made to obtain and reduce the crystallographic data and also to solve and refine the structures is given separately under the name of each compound.

$[(p_3)NiSNi(p_3)](BPh_4)_2 \cdot 1.6DMF$. From the analysis of the orientation matrix **UB** and the reciprocal matric tensor **M** (**M** = **UB·UB**) the lattice was identified as triclinic. Successful refinement of the structure in the space group $P\bar{1}$ indicated that the hypothesis of a centrosymmetric structure was correct. The cell constants, determined by least-squares refinement of the setting angles of 20 orienting reflections, are $a = 17.754$ (4) Å, $b = 13.972$ (3) Å, $c = 12.658$ (3) Å, $\alpha = 93.09$ (2)°, $\beta = 106.41$ (2)°, and $\gamma = 106.89$ (2)°. A density of 1.194 g cm^{-3} calculated for one unit formula of $C_{136}H_{150}N_2O_2B_2SP_6Ni_2$ in the cell agrees with the value of 1.18 g cm^{-3} obtained by flotation. The small, dark brown crystal chosen for data collection had faces of the form {100}, {001}, {011}, $\{01\bar{1}\}$. The separations between centrosymmetric pairs of faces were as follows: {100}, 0.0032 cm; {011}, 0.0266 cm; $\{01\bar{1}\}$, 0.0384 cm; {001}, 0.0148 cm; the crystal volume was 0.001 97 mm^3.

The data were collected by the θ–2θ scan technique at a scan rate of 0.04°/s. A scan width of 0.90° in θ (corrected for dispersion) was used throughout data collection. Stationary-counter, stationary-crystal background counts of a number of seconds equal to half of the peak scanning time were taken at each end of the scan. A unique data set, up to $\theta = 20°$, was gathered. A total of 4552 independent reflections were recorded. The intensities of three standard reflections, monitored every 2 h, showed only the deviations from the mean

0020-1669/78/1317-0632$01.00/0

Table I. Analytical and Physical Data of the Complexes

		% calcd					% found					
Compd	Color	C	H	M	N	S	C	H	M	N	S	μ_{eff}, μ_B[b]
$[(p_3)NiSNi(p_3)](BPh_4)_2\cdot 1.6DMF$[a]	Green	75.15	6.04	5.45	1.04	1.49	75.56	5.90	5.35	1.09	1.54	Diam
$[(np_3)CoSCo(np_3)]$	Brown	69.21	5.81	8.09	1.92	2.20	69.23	6.06	7.70	1.84	2.12	Diam
$[Ni(SH)(np_3)]$	Brown	67.66	5.81	7.88	1.88	4.30	67.35	5.67	7.85	1.83	4.25	1.92
$[Ni(SeH)(np_3)]$	Brown	63.66	5.47	7.41	1.77		63.93	5.41	7.60	1.73		1.92
$[Ni(SCH_3)(np_3)]$	Brown	68.00	5.97	7.73	1.84	4.22	68.46	6.17	7.40	1.76	4.01	1.92

[a] Calcd: P, 8.62. Found: P, 8.49. [b] 293 K.

Table II. Maxima and Extinction Coefficients for the Electronic Spectra of the Complexes

Compd		Absorption max, μm^{-1} (ϵ_M for soln)
$[(p_3)NiSNi(p_3)](BPh_4)_2\cdot$	a	0.90 sh, 1.11 sh, 1.59, 2.13, 2.61
1.6DMF	b	1.11 sh, 1.59 (22 600), 2.13 (41 500), 2.70 (8640)
$[(np_3)CoSCo(np_3)]$[c]	a	0.74 sh, 0.97, 1.45 sh, 2.32 sh
$[Ni(SH_3)(np_3)]$[d]	a	1.00 sh, 1.39, 2.04 sh, 2.70
$[Ni(SeH)(np_3)]$[d]	a	1.00 sh, 1.39, 2.00 sh, 2.60 sh
$[Ni(SCH_3)(np_3)]$[d]	a	0.87 sh, 1.22, 1.80 sh, 2.60 sh

[a] Solid at room temperature. [b] 1,2-Dichloroethane solution. [c] The compound is almost insoluble. [d] The compound slowly decomposes in the solution even under an inert atmosphere.

predicted from counting statistics.

Data processing was carried out as previously described.[9] A value of 0.04 was assigned to the instability factor R in the formula used to calculate the $\sigma(I)$'s. The values of I and $\sigma(I)$ were corrected for Lorentz–polarization and absorption effects. For the crystal chosen the transmission coefficients, evaluated by numerical integration, were found to range from 0.933 to 0.989 (linear absorption coefficients 4.84 cm^{-1}). Reflections totaling 1807 were greater than 3 times their estimated standard deviations and were used for the determination and refinement of the structure.

From a three-dimensional Patterson map Ni, P, and S atomic species in the asymmetric unit were located. F_c's calculated thereafter gave a value of the agreement factor $R_1 = \sum||F_o| - |F_c||/\sum|F_o|$ equal to 0.44. Two subsequent F_o Fourier syntheses were sufficient to detect the positions of all other nonhydrogen atoms except those belonging to the DMF molecule. Two cycles of full-matrix, isotropic least-squares refinement, using for the 10 phenyl groups in the asymmetric unit the rigid-body refinement routine of XRY72's CRYLSQ program, made operative in this laboratory, yielded values of R_1 and R_2 [$R_2 = (\sum w(|F_o| - F_c|)^2/\sum wF_o^2)^{1/2}$ with $w = 1/\sigma(F_o)$] of 0.129 and 0.172, respectively. It has been recently shown[10] that the geometry of substituted-benzene derivatives is sensitive to the nature of the substituent. Accordingly, concerning the constrained geometry imposed on the phenyl rings, a subtle distinction was made between rings attached to phosphorus atoms and rings attached to boron atoms. While D_{6h} geometry was kept for the former type of rings (C–C distance 1.392 Å, C–H distance 0.95 Å), the model indicated in ref 10b for boron-monosubstituted-benzene derivatives was employed in the latter case. In any case single isotropic thermal parameters were refined for carbon atoms.

A ΔF map enabled us to reveal the shape of the DMF molecule. Hydrogen atoms were also introduced at calculated positions. The Ni, S, and P atoms were assigned anisotropic thermal parameters and a least-squares cycle lowered R_1 and R_2 to 0.082 and 0.093, respectively. In this cycle the population parameters of atoms of DMF molecule were set equal to 1 and not varied. Due to the abnormal increase of the thermal parameters of these atoms a new ΔF map was prepared from which it was evident that (1) the electron density associated with the carbon atoms of this molecule was about two-thirds of that corresponding to a carbon atom of the cation and (2) the oxygen atom of the aldehydic group was distributed over two different positions. A subsequent least-squares cycle, run over the atomic parameters of the DMF molecule only, keeping all other parameters constant, lowered R_1 and R_2 to 0.075 and 0.083, respectively; in this cycle the population parameters of the carbon and nitrogen atoms were fixed at 0.8 (a value very close to the results of the elemental analysis) while the population parameters of the two possible locations of the oxygen atom were varied, but their sum was constrained to be 0.8. Finally a least-squares cycle was run over 211 variables contemporaneously. No shift per error was larger than 0.9 and refinement was then considered terminated. The error in an observation of unit weight is 1.34 e.

The present values of R_1 and R_2 are 0.066 and 0.072.

In Tables III–VI the final atomic parameters are reported.

[(np$_3$)CoSCo(np$_3$)]. In contrast to the behavior of the nickel compound, this complex is moderately air unstable and highly unstable under x radiation; hence its study with diffraction methods proved quite difficult.

A small crystal (0.2 × 0.06 × 0.06 mm^3), whose shape was that of a very elongated rhombohedron, was studied on the diffractometer with the above described techniques. A set of 15 orienting reflections led to refined cell parameters a = 23.204 (4) Å, b = 13.400 (3) Å, c = 27.931 (5) Å, and β = 123.58 (4)°. The density of 1.33 g cm^{-1} calculated for four unit formulas of $C_{84}H_{72}N_2P_6SCo_2$ in the cell well agrees with the measured value of 1.32 g cm^{-1}. After the examination of the systematic absences and from the indication derived from the density, the monoclinic space group C_2/c was chosen. Only at a later stage of the structure determination (see below) was the actual higher symmetry (rhombohedral) of the crystal recognized after a reexamination of the whole process of the lattice's determination and the cell's reduction. The following matrices were derived which conform, respectively, to the transformation matrices **I** and **II** which are defined

$$\underset{\mathbf{I}}{\begin{pmatrix} 0.5 & -0.5 & 1 \\ 0.5 & 0.5 & 1 \\ 1 & 0 & 1 \end{pmatrix}} \qquad \underset{\mathbf{II}}{\begin{pmatrix} -1 & -1 & 2 \\ -1 & 1 & 0 \\ 1 & 1 & -1 \end{pmatrix}}$$

in ref 11 and which allow a ready transformation of all covariant and controvariant quantities from the monoclinic to the rhombohedral cell and vice versa. Consequently the new rhombohedral cell parameters are a = 24.505 (4) Å and α = 31.71 (3)°; the volume of the cell (3615 Å^3) is half that of the monoclinic cell and likewise for the number of formula units in the cell. The space group was found to be $R\bar{3}c$. Actually, the data were collected as if the crystal were monoclinic and the structure was solved in this system. Only the final refinement was made in the higher symmetry system. The use of the old set of data was preferred to a new data collection on a sample which was difficult to crystallize in suitable-sized crystals and which was so difficult to handle experimentally.

For data collection the θ–2θ scan technique was used at a scan rate of 0.07°/s over a scan width of 0.8° in θ (corrected for dispersion).

Table III. Atomic Parameters (×10^4) for the Structure of $[(p_3)NiSNi(p_3)](BPh_4)_2\cdot 1.6DMF$[a]

Atom	x	y	z	U_{11}	U_{22}	U_{33}	U_{12}	U_{13}	U_{23}
Ni	966 (2)	1166 (2)	1008 (2)	423 (19)	331 (18)	354 (18)	93 (15)	101 (14)	56 (14)
P1	1018 (3)	2765 (4)	838 (4)	507 (43)	404 (39)	364 (37)	108 (34)	86 (32)	56 (32)
P2	2254 (3)	1453 (4)	943 (4)	375 (39)	426 (40)	435 (39)	158 (32)	57 (30)	61 (31)
P3	1423 (3)	1472 (4)	2874 (4)	518 (43)	392 (39)	441 (39)	87 (32)	154 (32)	115 (31)
S	0	0	0	496 (58)	486 (56)	519 (56)	180 (46)	173 (45)	127 (44)

[a] The form of the thermal ellipsoid is $\exp(-2\pi^2(U_{11}h^2a^{*2} + U_{22}k^2b^{*2} + U_{33}l^2c^{*2} + 2U_{12}hka^*b^* + \ldots))$. F (relative scale factor) = 64 786.

Table IV. Atomic Parameters ($\times 10^3$) for the Structure of $[(p_3)NiSNi(p_3)](BPh_4)_2 \cdot 1.6DMF$

Atom	*x*	*y*	*z*	*U*, Å^2
C1	193 (1)	362 (1)	191 (1)	52 (6)
C2	293 (1)	271 (1)	174 (1)	54 (6)
C3	237 (1)	258 (1)	337 (1)	48 (6)
C4	263 (1)	325 (1)	252 (1)	41 (6)
C5	335 (1)	416 (1)	322 (2)	55 (6)
B	369 (1)	695 (2)	618 (2)	41 (7)
O1[a,b]	279 (2)	590 (2)	124 (2)	107 (11)
O2[a,c]	343 (5)	541 (6)	84 (6)	186 (33)
C6[a,d]	361 (2)	650 (3)	144 (3)	134 (14)
C7[a,d]	332 (2)	663 (3)	−49 (3)	148 (15)
C8[a,d]	441 (2)	771 (3)	75 (3)	125 (12)
N1[a,d]	372 (1)	682 (2)	56 (2)	80 (8)

[a] Atoms belonging to the DMF molecule. [b] Refined population parameter 0.53. [c] Refined population parameter 0.27. [d] Constrained population parameter 0.80.

Background measurements were made as in the previous compound. Up to $\theta = 23°$ a total number of 5482 reflections were measured, the greatest number of observed reflections being in the shell limited at $\theta = 18°$. Decomposition of the specimen as observed from the decay of the intensities of three standard reflections monitored every 2 h reached up to 22% at the end of the collection of the first shell and up to 35% at the completion of data collection. A linear correction factor for decomposition was applied to the intensity data. Data reduction was performed as for the previous compound but no absorption correction was applied in view of the small size of the specimen (linear absorption coefficient 6.61 cm^{-1}).

The structure was solved from Patterson and Fourier methods using 762 reflections with intensities greater than $3\sigma(I)$ and belonging to the first shell. After the location of the sulfur, cobalt, and all of the nonhydrogen atoms of the np$_3$ ligand, isotropic least-squares refinement using rigid-body models for the phenyl rings lowered R_1 to 0.18. Introduction of anisotropic temperature factors for heavier atoms did not improve the model decisively. It was at this point that a reexamination of all the data led to the discovery of the rhombohedral symmetry. Using matrix **I** the new indices were derived and equivalent reflections were averaged. This process reduced the number of independent reflections to 424 (all data available up to $\theta = 23°$ being included). By use of the transpose of matrix **II** new coordinates were also derived from those obtained in the monoclinic cell and an asymmetric set of Co, S, and N atoms was located on a threefold axis, the sulfur atom in particular being at point symmetry 32. The subsequent least-squares refinement using anisotropic temperature factors for Co, S, and P atoms and the unconstrained model for the phenyl groups lowered R_1 and R_2 factors to 0.079 and 0.069, respectively. A final least-squares cycle after the introduction of hydrogen atoms at calculated positions gave $R_1 = 0.065$ and $R_2 = 0.055$. The standard deviation of an observation of unit weight is 3.87 e.

In Tables VII and VIII the final atomic parameters are reported. Observed and calculated structure factors of both structures which were used in the refinements are available as supplementary material.

Results and Discussion

The formation of complex $[(p_3)NiSNi(p_3)](BPh_4)_2$ can be attributed to the considerable acidity displayed by H_2S following coordination and to the basicity of the tertiary phosphine groups of the ligand p$_3$[9] which can bind hydrogen ions with the formation of quaternary phosphonium ions of the form p_3H^+, etc. Consequently, the general reaction can be written

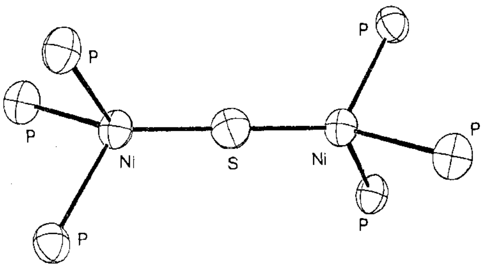

Figure 1. Inner skeleton of the complex cation $[(p_3)NiSNi(p_3)]^{2+}$.

$$2[Ni(H_2O)_6]^{2+} + p_3(\text{excess}) + H_2S \rightarrow [(p_3)NiSNi(p_3)]^{2+} + 2p_3H^+ + 6H_2O$$

The formation of the complex $[(np_3)CoSCo(np_3)]$ can be attributed to the action of sodium ethoxide which both neutralizes the H_2S liberated during the condensation of the complex $[Co(SH)(np_3)]^+$ and reduces the metal according to the reaction

$$2[Co(SH)(np_3)]BPh_4 + 4NaOC_2H_5 \rightarrow [(np_3)CoSCo(np_3)] + 2NaBPh_4 + Na_2S + 2C_2H_5OH + 2CH_3CHO + H_2$$

The reactions which lead to the formation of the nickel(I) complexes can be considered as oxidative additions of H_2S, $HSCH_3$, or H_2Se to the trigonal-bipyramidal complex of nickel(0) $[Ni(np_3)]$ with elimination of hydrogen according to the general reaction

$$[Ni(np_3)] + HXR \rightarrow [Ni(XR)(np_3)] + {}^1/{}_2H_2$$
$$(X = S;\ R = H, CH_3;\ X = Se,\ R = H)$$

The dimeric complex of nickel(II) is stable in air, either in the solid state or in solution. The complexes of the metals in oxidation state +1, especially that of cobalt, decompose slowly in air. The three nickel(I) complexes slowly decompose in solutions of polar solvents, even under an inert atmosphere.

The thio complex of nickel(II) has in nitroethane a molar conductance indicative of a 1:2 electrolyte (114 cm^2 Ω^{-1} mol^{-1}).

The two thio complexes of cobalt(I) and nickel(II) are diamagnetic. The nickel(I) complexes have magnetic moments at room temperature typical of a d^9 configuration ($\mu_{\text{eff}} = 1.92$ μ_B, Table I).

The solid-state structure of the nickel complex **1** consists of dimeric cations and tetraphenylborate anions, a nonstoichiometric amount of DMF also being present in the cell. Figure 1 shows the skeleton of the complex; a stereoscopic view of the whole molecule is presented in Figure 2. Selected

Table V. Final Least-Squares Parameters for $[(p_3)NiSNi(p_3)](BPh_4)_2 \cdot 1.6DMF$ Groups[a]

Group	x'	y'	z'	θ	ϕ	ψ
1	0.1104 (6)	0.3304 (6)	−0.1399 (7)	1.717 (10)	1.180 (10)	2.523 (10)
2	−0.0382 (5)	0.3344 (7)	0.1217 (6)	2.920 (7)	1.046 (15)	−1.849 (12)
3	0.2480 (6)	0.1562 (6)	−0.1294 (8)	1.486 (11)	2.026 (10)	−0.347 (18)
4	0.2944 (5)	−0.0169 (7)	0.1816 (7)	2.025 (9)	0.382 (10)	1.214 (10)
5	0.1934 (5)	−0.0211 (7)	0.3959 (7)	1.223 (10)	2.677 (9)	−1.906 (10)
6	0.0197 (6)	0.1867 (8)	0.3922 (6)	0.395 (8)	1.294 (12)	1.957 (6)
7	0.3914 (6)	0.8833 (7)	0.7789 (7)	2.427 (9)	−1.709 (11)	−0.538 (13)
8	0.1897 (6)	0.6029 (6)	0.4688 (8)	1.675 (9)	−0.621 (10)	2.689 (9)
9	0.4871 (5)	0.7538 (7)	0.4810 (6)	0.590 (7)	1.646 (13)	1.074 (10)
10	0.4193 (6)	0.5340 (8)	0.7561 (8)	1.318 (10)	−2.426 (12)	−1.165 (8)

[a] x', y', and z' (fractional coordinates) define the origin of the working system of the group. The Goldstein definition is used for Euler angles θ, ϕ, and ψ (radians): H. Goldstein, "Classical Mechanics", Addison-Wesley, Reading, Mass., 1959.

Table VI. Thermal and Derived Positional Parameters ($\times 10^3$) of Group Atoms

Atom	x	y	z	U, Å^2
C1 1[a]	109 (1)	313 (1)	−49 (1)	40 (5)
C2 1	182 (1)	373 (1)	−64 (1)	65 (7)
C3 1	184 (1)	393 (1)	−170 (1)	76 (7)
C4 1	112 (1)	353 (1)	−261 (1)	82 (8)
C5 1	39 (1)	294 (1)	−246 (1)	88 (8)
C6 1	38 (1)	274 (1)	−140 (1)	74 (7)
C1 2	16 (1)	310 (1)	103 (1)	41 (6)
C2 2	−49 (1)	238 (1)	125 (1)	70 (7)
C3 2	−112 (1)	267 (1)	147 (1)	79 (7)
C4 2	−111 (1)	368 (1)	147 (1)	100 (9)
C5 2	−46 (1)	439 (1)	125 (1)	78 (7)
C6 2	17 (1)	410 (1)	103 (1)	59 (6)
C1 3	238 (1)	148 (1)	−40 (1)	48 (6)
C2 3	318 (1)	187 (1)	−48 (1)	81 (7)
C3 3	329 (1)	196 (1)	−152 (1)	96 (8)
C4 3	261 (1)	166 (1)	−248 (1)	83 (8)
C5 3	182 (1)	128 (1)	−240 (1)	79 (7)
C6 3	170 (1)	119 (1)	−137 (1)	65 (7)
C1 4	271 (1)	51 (1)	148 (1)	51 (6)
C2 4	330 (1)	67 (1)	252 (1)	58 (6)
C3 4	358 (1)	−13 (1)	291 (1)	60 (6)
C4 4	325 (1)	−108 (1)	226 (1)	75 (7)
C5 4	266 (1)	−123 (1)	122 (1)	87 (8)
C6 4	239 (1)	−44 (1)	83 (1)	68 (7)
C1 5	170 (1)	44 (1)	354 (1)	49 (6)
C2 5	224 (1)	65 (1)	463 (1)	58 (6)
C3 5	251 (1)	−12 (1)	512 (1)	70 (7)
C4 5	224 (1)	−108 (1)	452 (1)	58 (6)
C5 5	171 (1)	−129 (1)	343 (1)	62 (7)
C6 5	144 (1)	−52 (1)	294 (1)	57 (6)
C1 6	72 (1)	175 (1)	355 (1)	55 (6)
C2 6	73 (1)	272 (1)	387 (1)	69 (7)
C3 6	12 (1)	286 (1)	430 (1)	75 (7)
C4 6	−50 (1)	203 (1)	441 (1)	87 (8)
C5 6	−51 (1)	106 (1)	409 (1)	100 (8)
C6 6	10 (1)	91 (1)	366 (1)	96 (8)
C1 7	377 (1)	796 (1)	701 (1)	46 (6)
C2 7	456 (1)	861 (1)	761 (1)	77 (7)
C3 7	470 (1)	945 (1)	836 (1)	94 (8)
C4 7	405 (1)	967 (1)	854 (1)	83 (8)
C5 7	326 (1)	907 (1)	798 (1)	79 (7)
C6 7	313 (1)	823 (1)	724 (1)	64 (6)
C1 8	275 (1)	645 (1)	538 (1)	53 (6)
C2 8	209 (1)	604 (1)	580 (1)	67 (7)
C3 8	128 (1)	564 (1)	514 (1)	91 (8)
C4 8	108 (1)	563 (1)	402 (1)	78 (8)
C5 8	169 (1)	601 (1)	355 (1)	80 (7)
C6 8	250 (1)	641 (1)	423 (1)	65 (7)
C1 9	433 (1)	727 (1)	547 (1)	50 (6)
C2 9	451 (1)	820 (1)	508 (1)	65 (7)
C3 9	503 (1)	846 (1)	444 (1)	77 (7)
C4 9	540 (1)	779 (1)	417 (1)	76 (7)
C5 9	524 (1)	687 (1)	453 (1)	87 (8)
C6 9	472 (1)	663 (1)	516 (1)	74 (7)
C1 10	395 (1)	609 (1)	694 (1)	46 (6)
C2 10	464 (1)	633 (1)	789 (1)	111 (9)
C3 10	488 (1)	561 (1)	849 (1)	110 (9)
C4 10	443 (1)	461 (1)	816 (1)	99 (8)
C5 10	374 (1)	433 (1)	724 (1)	100 (9)
C6 10	351 (1)	506 (1)	665 (1)	74 (7)

[a] Group numbers.

intramolecular bond distances and angles are reported in Tables IX and X. The complex has a crystallographically imposed center of symmetry which is the site of an unprecedented sulfur atom linearly bridging the two metal ions. Each nickel atom is bound to three phosphorus atoms of the p_3 ligand, a distorted tetrahedral geometry thus being completed. The two tetrahedra are rotated by about 60° with respect to each other, the resulting symmetry of the complex being approximately D_{3d}. The three Ni–P distances as well as the P–Ni–P angles are practically equal within standard deviations (average values of 2.236 Å and 92.39°, respectively). The most evident deviations from the assumed ternary symmetry of the complex is found for the angle S–Ni–P_3 (128.34 (18)°) which is larger than the other two S–Ni–P magnitudes (121.47 (16) and 121.67 (19)°, respectively). Noteworthy is the Ni–S bond distance (2.034 (2) Å) which is the shortest ever found for such a linkage in transition-metal complexes.[12]

The shape of the cobalt complex **2** is shown in Figure 3. The rhombohedral cell contains two molecules of the uncharged $[Co_2(np_3)]_2S$ complex lying parallel with the cell's threefold axis. Independent intramolecular bond distances and angles are reported in Table XI. The coordination about each metal atom is nearly tetrahedral in this case as well. The three phosphorus atoms of each ligand np_3 are bound to the cobalt ion at a distance of 2.285 (9) Å, the angle P–Co–P being 100.73 (17)°. The sulfur atom completes the two tetrahedra by bridging linearly the two cobalt atoms at 2.128 (1) Å. The angle S–Co–P has a value of 117.22 (13)°. The nitrogen atom is not linked to the metal (Co–N distance 3.485 (8) Å). The symmetry of the skeleton of the dimeric chromophore is D_{3h}. The Co–N distance in this complex is much longer than that in all the tetrahedrally distorted trigonal-bipyramidal Co(II) complexes with the same ligand np_3 and even longer than that (3.18 Å) found in the tetrahedral nitrosyl complex $[Ni(NO)(np_3)]^+$.[13]

As a final remark the Co–S distance in complex **2** is higher by about 0.1 Å than the Ni–S distance in complex **1**. Such a difference may be attributed both to the Ni(II) ionic radius, which is shorter than that of Co(I), and to repulsive forces between phenyl rings of the ligands which are allegedly higher in the eclipsed rather than in the staggered configuration.

The electronic spectra of the two d^8 metal dimeric compounds, showing several absorption edges in the range 0.75–2.70 μm^{-1} (Table II), are comparable but are not easily interpretable in the absence of more detailed studies.

The electronic spectra of the nickel(I) complexes are all similar with three main absorptions at 1.00–1.40, 1.80–2.04, and 2.60–2.75 μm^{-1} and are fully comparable with those of the complexes $[NiX(np_3)]$ (X = Cl, Br, I) having a trigonal-bipyramidal geometry.[6]

The IR spectrum of the $[Ni(SH)(np_3)]$ complex exhibits a very weak absorption at 2545 cm^{-1} attributable to the ν(SH) stretching vibration; the corresponding ν(SeH) absorption appears in the IR spectrum of the hydrogenselenido complex $[Ni(SeH)(np_3)]$ at 2270 cm^{-1}.

It remains now to explain the diamagnetism of the two binuclear complexes in which a sulfur atom bridges linearly two d^8 metal ions which have tetrahedral coordination. Since the two individual d^8 entities would be paramagnetic, it seems probable that a superexchange mechanism through the sulfur atom, utilizing p_π orbitals of the sulfur and orbitals of higher energy of the metal (symmetry D_{3d} or D_{3h}), is involved. This interaction (which must be introduced to account for the

Table VII. Atomic Parameters ($\times 10^4$) for the Structure of $[(np_3)CoSCo(np_3)]$[a]

Atom	x	y	z	U_{11}	U_{22}	U_{33}	U_{12}	U_{13}	U_{23}
Co1	2805 (1)	2805 (1)	2805 (1)	435 (17)	435 (17)	435 (17)	−196 (9)	−196 (9)	−196 (9)
S1	2500	2500	2500	361 (43)	361 (43)	361 (43)	−168 (23)	−168 (23)	−168 (23)
P1	2946 (4)	4476 (5)	1443 (5)	406 (39)	654 (44)	660 (44)	−246 (36)	−145 (35)	−413 (38)

[a] The form of the thermal ellipsoid is $\exp(-2\pi^2(U_{11}h^2a^{*2} + U_{22}k^2b^{*2} + U_{33}l^2c^{*2} + 2U_{12}hka^*b^* + \ldots))$. F (relative scale factor) = 87 924.

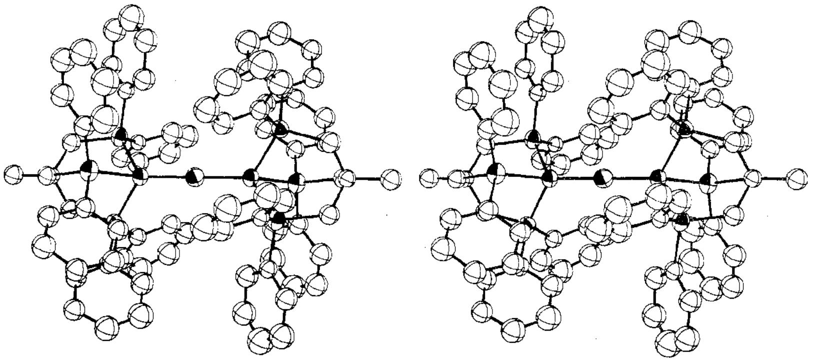

Figure 2. Stereoscopic view of the whole complex cation $[(p_3)NiSNi(p_3)]^{2+}$.

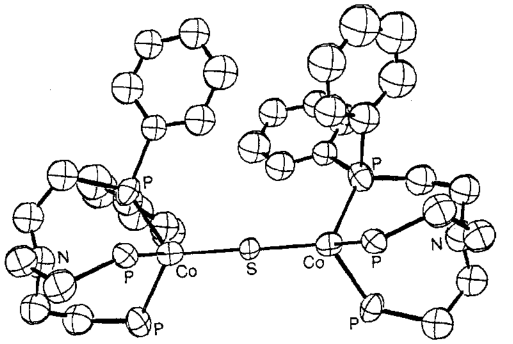

Figure 3. A view of the molecule of the complex $[(np_3)CoSCo(np_3)]$. For sake of clarity only the phenyl rings of each np_3 ligand not repeated by the threefold axis are shown.

Table VIII. Atomic Parameters (×10⁴) for the Structure of $[(np_3)CoSCo(np_3)]$

Atom		x	y	z	U, Å^2
N1		3305 (3)	3305 (3)	3305 (3)	685 (78)
C1		3760 (15)	4588 (14)	1245 (15)	725 (72)
C2		3314 (13)	4413 (13)	2312 (13)	690 (72)
C1	1[a]	1526 (22)	5785 (15)	1615 (21)	720 (57)
C2	1	580 (19)	5790 (16)	2157 (17)	716 (70)
C3	1	−544 (20)	6777 (24)	2279 (19)	995 (81)
C4	1	−620 (20)	7702 (21)	1836 (21)	1150 (90)
C5	1	240 (24)	7733 (19)	1367 (18)	1200 (101)
C6	1	1349 (25)	6785 (20)	1218 (22)	1051 (72)
C1	2	3587 (15)	5026 (16)	−113 (15)	498 (58)
C2	2	3850 (17)	5953 (19)	−1024 (20)	786 (79)
C3	2	4237 (15)	6341 (15)	−2094 (17)	630 (67)
C4	2	4345 (15)	6022 (17)	−2433 (16)	712 (64)
C5	2	4128 (16)	5079 (17)	−1542 (19)	897 (80)
C6	2	3721 (15)	4616 (15)	−386 (17)	698 (69)

[a] Group numbers.

Table IX. Selected Intramolecular Bond Distances (Å) for $[(p_3)NiSNi(p_3)](BPh_4)_2 \cdot 1.6DMF$

Ni–S	2.034 (2)	C1–C4	1.519 (28)
Ni–P1	2.233 (6)	C2–C4	1.510 (30)
Ni–P2	2.231 (6)	C3–C4	1.548 (27)
Ni–P3	2.243 (6)	C4–C5	1.534 (21)
P1–C1	1.829 (15)	B–C1(7)	1.661 (29)
P2–C2	1.850 (16)	B–C1(8)	1.620 (26)
P3–C3	1.846 (16)	B–C1(9)	1.609 (30)
P1–C1(1)[a]	1.811 (16)	B–C1(10)	1.657 (28)
P1–C1(2)	1.788 (17)	N1–C6	1.26 (5)
P2–C1(3)	1.784 (16)	N1–C7	1.29 (4)
P2–C1(4)	1.806 (16)	N1–C8	1.42 (4)
P3–C1(5)	1.829 (16)	C7–O1	1.38 (5)
P3–C1(6)	1.820 (17)	C7–O2	1.56 (9)

[a] Group numbers in parentheses.

Table X. Selected Intramolecular Bond Angles (deg) for $[(p_3)NiSNi(p_3)](BPh_4)_2 \cdot 1.6DMF$

Ni–S–Ni	180	P1–C1–C4	120.0 (1.3)
P1–Ni–P2	92.46 (22)	P2–C2–C4	119.3 (1.3)
P1–Ni–P3	93.54 (21)	P3–C3–C4	118.3 (1.1)
P2–Ni–P3	91.18 (21)	C1–C4–C5	108.0 (1.5)
P1–Ni–S	120.47 (16)	C2–C4–C5	108.6 (1.6)
P2–Ni–S	121.67 (19)	C3–C4–C5	105.0 (1.3)
P3–Ni–S	128.34 (18)	C1–C4–C2	113.1 (1.4)
Ni–P1–C1	109.66 (69)	C1–C4–C3	110.2 (1.6)
Ni–P2–C2	110.12 (75)	C2–C4–C3	114.4 (1.6)
Ni–P3–C3	110.75 (64)	C1(7)–B–C1(8)	110.0 (1.7)
Ni–P1–C1(1)[a]	114.57 (60)	C1(7)–B–C1(9)	109.0 (1.6)
Ni–P1–C1(2)	115.11 (63)	C1(7)–B–C1(10)	109.9 (1.6)
Ni–P2–C1(3)	116.30 (73)	C1(8)–B–C1(9)	111.5 (1.7)
Ni–P2–C1(4)	113.56 (71)	C1(8)–B–C1(10)	108.1 (1.6)
Ni–P3–C1(5)	114.44 (67)	C1(9)–B–C1(10)	108.3 (1.7)
Ni–P3–C1(6)	116.43 (67)		
C1–P1–C1(1)	106.8 (1.2)	C6–N1–C7	136.7 (2.8)
C1–P1–C1(2)	104.7 (1.1)	C6–N1–C8	114.6 (2.5)
C1(1)–P1–C1(2)	105.3 (1.2)	C7–N1–C8	108.2 (2.8)
C2–P2–C1(3)	104.6 (1.3)	N1–C7–O1	111.3 (2.9)
C2–P2–C1(4)	108.3 (1.3)	N1–C7–O2	87.4 (4.4)
C1(3)–P2–C1(4)	103.3 (1.2)	O1–C7–O2	68.1 (3.9)
C3–P3–C1(5)	105.1 (1.2)		
C3–P3–C1(6)	105.1 (1.3)		
C1(5)–P3–C1(6)	104.0 (1.2)		

[a] Group numbers in parentheses.

Table XI. Selected Intramolecular Bond Distances (Å) and Angles (deg) for $[(np_3)CoSCo(np_3)]$

Co–N1	3.485 (8)	S1–Co–S1	180
Co–S1	2.128 (1)	S1–Co–P1	117.22 (13)
Co–P1	2.285 (9)	P1–Co–P1′	100.73 (17)
P1–C1	1.830 (15)	Co–P1–C1	121.49 (60)
P1–C1(1)[a]	1.842 (18)	Co–P1–C1(1)	114.03 (71)
P1–C1(2)	1.870 (17)	Co–P1–C1(2)	117.42 (65)
C1–C2	1.498 (20)	C1–P1–C1(1)	102.1 (1.0)
N1–C2	1.438 (14)	C1–P1–C1(2)	99.4 (0.9)
C1(1)–C2(1)	1.372 (26)	P1–C1–C2	114.2 (0.9)
C2(1)–C3(1)	1.423 (27)	C1–C2–N1	113.1 (0.9)
C3(1)–C4(1)	1.337 (28)	C2–N1–C2′	116.0 (0.9)
C4(1)–C5(1)	1.331 (30)	C2(1)–C1(1)–C6(1)	117.9 (1.2)
C5(1)–C6(1)	1.390 (32)	C1(1)–C2(1)–C3(1)	122.5 (1.3)
C6(1)–C1(1)	1.412 (28)	C2(1)–C3(1)–C4(1)	115.4 (1.3)
C1(2)–C2(2)	1.408 (24)	C4(1)–C5(1)–C6(1)	119.8 (1.3)
C2(2)–C3(2)	1.319 (25)	C3(1)–C4(1)–C5(1)	125.3 (1.3)
C3(2)–C4(2)	1.324 (25)	C5(1)–C6(1)–C1(1)	118.9 (1.2)
C4(2)–C5(2)	1.388 (26)	C2(2)–C1(2)–C6(2)	117.8 (1.2)
C5(2)–C6(2)	1.401 (26)	C1(2)–C2(2)–C3(2)	117.8 (1.1)
C6(2)–C1(2)	1.328 (25)	C2(2)–C3(2)–C4(2)	128.2 (1.2)
		C3(2)–C4(2)–C5(2)	113.7 (1.2)
		C4(2)–C5(2)–C6(2)	120.9 (1.2)
		C5(2)–C6(2)–C1(2)	121.2 (1.1)

[a] Group numbers in parentheses.

diamagnetism of the complexes) will be favored by the linearity of the sulfur bridge and by the relatively low electronegativity of the sulfur atom.

Acknowledgment. Thanks are expressed to Mr. F. Cecconi, Mr. D. Masi, and Mr. F. Zanobini for technical assistance and to Mr. F. Nuzzi and Mr. G. Vignozzi for microanalysis.

Registry No. 1, 64998-75-0; **2**, 64938-99-4; [Ni(SH)(np$_3$)], 64939-17-9; [Ni(SeH)(np$_3$)], 64939-19-1; [Ni(SCH$_3$)(np$_3$)], 64939-21-5; [Ni(H$_2$O)$_6$](BF$_4$)$_2$, 14322-78-2; [Co(SH)(np$_3$)]BPh$_4$, 61966-76-5; Ni(np$_3$), 52633-73-5; H$_2$S, 7783-06-4; H$_2$Se, 7783-07-5; HSCH$_3$, 74-93-1.

Supplementary Material Available: Listings of observed and calculated structure factors for [(p$_3$)NiSNi(p$_3$)]·1.6DMF and [(np$_3$)CoSCo(np$_3$)](BPh$_4$)$_2$·1.6DMF (15 pages). Ordering information is given on any current masthead page.

References and Notes

(1) Part 1: M. Di Vaira, S. Midollini, and L. Sacconi, *Inorg. Chem.*, **16**, 1518 (1977).
(2) J. P. Collman, R. K. Rothrock, and R. A. Stark, *Inorg. Chem.*, **16**, 437 (1977); B. H. Vahrenkamp, *Angew. Chem., Int. Ed. Engl.*, **14**, 322 (1975).
(3) C. Mealli, S. Midollini, and L. Sacconi, *J. Chem. Soc., Chem. Commun.*, 765 (1975).
(4) W. Hewertson and H. R. Watson, *J. Chem. Soc.*, 1490 (1962).
(5) L. Sacconi and I. Bertini, *J. Am. Chem. Soc.*, **90**, 5443 (1968).
(6) L. Sacconi, C. A. Ghilardi, C. Mealli, and F. Zanobini, *Inorg. Chem.*, **14**, 1380 (1975).
(7) L. Sacconi and R. Morassi, *J. Chem. Soc. A*, 2997 (1968); L. Sacconi, I. Bertini, and F. Mani, *Inorg. Chem.*, **7**, 1417 (1968).
(8) *Philips Serving Science and Industry*, **18**, 22 (1972).
(9) C. Mealli, S. Midollini, and L. Sacconi, *Inorg. Chem.*, **14**, 2513 (1975).
(10) (a) A. Domenicano and A. Vaciago, *Acta Crystallogr., Sect. B*, **31**, 2553 (1975); (b) A. Domenicano, A. Vaciago, and C. A. Coulson, *ibid.*, **31**, 221 (1975); (c) A. Domenicano, A. Vaciago, and C. A. Coulson, *ibid.*, **31**, 1630 (1975).
(11) "International Tables for X-Ray Crystallography", Vol. I, N. F. M. Henry and K. Lonsdale, ed., Kynoch Press, Birmingham, England, 1966, pp 15–18.
(12) A Ni–S distance of 2.02 Å is reported for the mineral parkerite (Ni$_3$Bi$_2$S$_2$): M. E. Fleet, *Am. Mineral.*, **58**, 435 (1973).
(13) M. Di Vaira, C. A. Ghilardi, and L. Sacconi, *Inorg. Chem.*, **15**, 1555 (1976), and references therein.

Contribution from the Los Alamos Scientific Laboratory,
University of California, Los Alamos, New Mexico 87545

Lability and Reactivity of Sulfur Dioxide–Transition Metal Complexes: Crystal and Molecular Structure of OsHCl(CO)[P(C$_6$H$_{11}$)$_3$]$_2$(SO$_2$)·2CHCl$_3$

R. R. RYAN* and G. J. KUBAS

Received May 10, 1977

An x-ray structure determination of OsHCl(CO)(PCy$_3$)$_2$(SO$_2$)·2CHCl$_3$ (Cy = cyclohexyl) reveals octahedral coordination about the d^6 osmium(II) and a coplanar Os–SO$_2$ moiety with the hydride ligand presumably occupying the site trans to the SO$_2$. The long Os–S bond length (2.239 (3) Å) in comparison to those previously found for coplanar M–SO$_2$ groups is indicative of the strong trans influence of the hydride. The latter is also manifested by the unexpected reversibility of the metal–SO$_2$ interaction and the reaction of the complex with oxygen in solution to yield an Os(III) sulfato species, OsCl(CO)(PCy$_3$)$_2$(SO$_4$). The structure of the SO$_2$ adduct shows disorder between the chloride and carbonyl, which has been partially resolved. Important distances and angles are Os–P = 2.421 (3) and 2.425 (3) Å, Os–Cl = 2.43 (2) Å (average), Os–C = 1.93 (4) Å (average), S–O = 1.43 (1) and 1.44 (1) Å, O–S–O = 112.9 (6)°, P–Os–S = 102.9 (1) and 100.6 (1)°, and P–Os–P = 156.4 (1)°. Cell data: space group, triclinic; $Z = 2$; $a = 19.501$ (9), $b = 14.483$ (5), $c = 10.868$ (4) Å; $\alpha = 70.20$ (2), $\beta = 109.86$ (2), $\gamma = 120.96$ (2)°; $R = 0.055$ for 4450 diffractometer-collected reflections with $I \geq 3\sigma(I)$.

Introduction

A five-coordinate osmium(II) complex, OsHCl(CO)(PCy$_3$)$_2$ (Cy = cyclohexyl), has recently been synthesized and found to take up SO$_2$, presumably as a sixth ligand to the metal.[1] The reported positions of the SO infrared stretching frequencies (1284 and 1109 cm^{-1}) indicated the MSO$_2$ geometry to be coplanar by comparisons with frequencies reported for known examples of the geometry.[2] On the basis of previously reported d^6, six-coordinate complexes of transition metals containing SO$_2$ as a ligand [i.e., [Ru(NH$_3$)$_4$(SO$_2$)Cl]Cl[3] and Mn(C$_5$H$_5$)(CO)$_2$(SO$_2$)[4]] we expected[5] the present complex to contain a coplanar Os–SO$_2$ moiety with a nonlabile SO$_2$ group inert to attack by molecular oxygen (see also ref 6 and 7 concerning Rh(C$_5$H$_5$)(C$_2$H$_4$)(SO$_2$) and Ni(p$_3$)SO$_2$). Since studies of the reactivity of coordinated SO$_2$ are still in an embryonic stage, we decided to further examine the properties of this complex as part of our general investigation into the bonding of SO$_2$ to metal complexes. The results of this study, including the x-ray determination of the structure, are reported below.

Experimental Section

OsHCl(CO)(PCy$_3$)$_2$(SO$_2$)·C$_6$H$_6$ was prepared according to the published procedure.[1] Infrared spectra were recorded on a Perkin-Elmer 521 using Nujol mulls between CsBr plates. Elemental analyses were performed by Galbraith Laboratories, Inc., Knoxville, Tenn. Thermogravimetric analyses were carried out on a Perkin-Elmer TGS-2 using a nitrogen purge and a heating rate of 1.25°/min.

Reversibility of the OsHCl(CO)(PCy$_3$)$_2$–SO$_2$ Interaction. OsHCl(CO)(PCy$_3$)$_2$(SO$_2$)·C$_6$H$_6$ was heated on a vacuum line to 140 °C for 1 h, during which time the color of the complex changed from yellow to red-orange. Both benzene and SO$_2$ were identified by mass spectroscopy to be present in the evolved volatiles, which were trapped at −196 °C using standard vacuum line techniques (molar ratio of volatiles/complex = 1.84). Furthermore, gaseous SO$_2$ could be readded (300 Torr, 30 min) to the red-orange residue, identified to be OsHCl(CO)(PCy$_3$)$_2$, to yield yellow OsHCl(CO)(PCy$_3$)$_2$(SO$_2$) in quantitative yield. Repetition of the SO$_2$ removal and readdition steps clearly indicated that the Os–SO$_2$ interaction is completely reversible, as had been found[8] for the M–SO$_2$ interaction in MCl(CO)(PPh$_3$)$_2$(SO$_2$) (M = Ir, Rh).

Reaction of OsHCl(CO)(PCy$_3$)$_2$(SO$_2$) with Oxygen to Give OsCl(CO)(PCy$_3$)$_2$(SO$_4$). Although the osmium–SO$_2$ adduct is air-stable in the solid state, its solutions readily air-oxidize to a sulfate complex. Saturation of a benzene solution (~20 mL) of OsHCl(CO)(PCy$_3$)$_2$(SO$_2$)·C$_6$H$_6$ (0.5 g) with oxygen resulted in slow precipitation of a light yellow solid beginning about 5 min after addition and continuing over a 3-day period. During this time the color of the supernatant solution underwent a series of dramatic color changes from yellow to gray-green to deep violet. The precipitate was collected, washed with benzene, and dried in vacuo at ambient temperature. Yield was 0.27 g (50%). The infrared spectrum of the solid revealed the presence of bidentate sulfate[9] (ν_{SO_4} 1283 (broad), 1165, 911, 890, 653, 603 cm^{-1}), carbonyl (ν_{CO} 1980 cm^{-1}), and lattice benzene ($\nu_{C_6H_6}$ 674 cm^{-1}). However, a metal–hydride stretch, which occurs at 2145 cm^{-1} for OsHCl(CO)(PCy$_3$)$_2$(SO$_2$)·C$_6$H$_6$,[1] was completely absent, indicating that the hydride ligand was displaced in the oxidation process.

The sulfate is nearly insoluble in benzene but very soluble in chloroform and was recrystallized from CHCl$_3$–hexane. CHCl$_3$ is retained in the crystal lattice very tightly (ν_{CHCl_3} 745 cm^{-1}) and cannot be completely removed even at 100 °C in vacuo. Elemental analysis revealed the empirical formula of the sulfate (dried at 100 °C) to be OsCl(CO)(PCy$_3$)$_2$(SO$_4$)·0.38CHCl$_3$. Anal. Calcd for

0020-1669/78/1317-0637$01.00/0 © 1978 American Chemical Society